# High-Quality Waveguide Bragg Gratings in Planar Lightwave Circuits Fabricated by Femtosecond Laser Direct Writing

Jiajun Guan, Zhihao Cai, Haoqiang Huang, Weijia Bao, Dejun Liu, Ying Wang, Cailing Fu, Jun He, *Member, IEEE*, Yiping Wang, *Senior Member, IEEE, Fellow, Optica*, and Changrui Liao, *Member, IEEE*

***Abstract*—This research pioneers the application of a femtosecond laser Burst-Mode technique for the fabrication of waveguide Bragg gratings (WBGs) within planar lightwave circuits (PLCs). Distinguished by its advantages in miniaturization, integration, and low loss, PLC technology emerges as a promising frontier in optical advancements. Our method significantly mitigates permanent damage to waveguides by employing lower pulse energy for multiple exposures at the same location, thereby enhancing the spectral properties of PLC-WBGs. Through meticulous exploration of the grating order's impact on WBG subpeaks, we refined our parameter optimization process. This led to the successful creation of a first-order WBG utilizing the femtosecond laser Burst-Mode technique, which yielded an outstanding return loss of approximately 32 dB. Further, we innovated upon this technique by integrating it with geometric apodization. Maintaining consistent grating length and laser energy parameters allowed for the fabrication of a double-apodized PLC-WBG, which introduced greater refractive index modulation (RIM) and achieved a Bragg resonance attenuation of roughly 12 dB and a side-mode suppression ratio (SMSR) of about 18 dB. Moreover, we developed stress waveguides adjacent to the core using the femtosecond laser, incorporating stressors with WBG. This innovation produced a WBG with significantly low birefringence of $5.66 \times 10^{-6}$ and a minimal polarization-dependent loss (PDL) of 0.8 dB. The high-quality WBGs fabricated through these advanced techniques offer vast potential for applications across diverse fields, such as multi-parameter sensing, optical communication systems, and fiber lasers.**

***Index Terms*—Burst-mode, femtosecond laser micromachining, planar lightwave circuit, waveguide Bragg gratings.**

## I. Introduction

THE planar lightwave circuit (PLC) exhibits advantages such as miniaturization, integration, and low loss, making it a highly promising device. It can be developed into a photonic integrated chip and applied across various domains, including optical communication, sensing, and computing [1], [2], [3]. Owing to its exceptional performance characteristics, it has garnered widespread attention. In 2006, Kim et al. integrated a Fabry-Perot laser diode (FP-LD) and Bragg grating in a PLC, proposing a highly linearly polarized external cavity laser [4]. Due to its excellent mode stability, it can be employed as a low-cost, high-spec degree source in optical communication networks. In 2007, Lee et al. introduced a dual-wavelength laser, utilizing hybrid integration of FP-LD and sampled Bragg grating in a silicon PLC, capable of generating terahertz beat signals [5]. In the same year, Song et al. presented an integrated optical transceiver employing thin-film filters (TFF) and waveguide Bragg grating (WBG), integrated with germanium-doped silica PLC, applicable to FTTX networks [6]. Additionally, in 2016, Zhang et al. utilized a PLC-based WBG for PON monitoring [7]. The encoding scheme exhibits various low-cost applications and excellent performance, offering a pathway for PON monitoring in the construction of smart cities. In these applications, WBGs prepared using the ultraviolet (UV) phase mask method based on PLC exhibit superior characteristics. Nevertheless, traditional UV laser fabrication of WBGs suffers from poor thermal stability, susceptibility to erasure under high-temperature conditions, and the need for cumbersome hydrogen loading pre-treatment, making it challenging to meet the demands of applications in extreme environments [8]. Furthermore, the fixed period of the phase mask limits the flexibility in fabricating wavelength division multiplexing (WDM)-FBG arrays. With the rapid advancement of femtosecond laser technology, exploring advanced techniques capable of directly writing high-quality WBGs in PLCs has become imperative.

Received 22 September 2024; revised 21 December 2024; accepted 28 December 2024. Date of publication 31 December 2024; date of current version 16 April 2025. This work was supported in part by the National Key Research and Development Program of China under Grant 2024YFB3213700, in part by the Shenzhen Science and Technology Program (Shenzhen Key Laboratory of Ultrafast Laser Micro/Nano Manufacturing under Grant ZDSYS20220606100405013), in part by the Natural Science Foundation of Guangdong Province under Grant 2022B1515120061, in part by the National Natural Science Foundation of China under Grant T2421003, in part by the Research Team Cultivation Program of Shenzhen University under Grant 2023QNT009. *(Corresponding author: Yiping Wang.)*

Jiajun Guan, Zhihao Cai, Haoqiang Huang, Weijia Bao, Dejun Liu, Ying Wang, Cailing Fu, Jun He, and Changrui Liao are with the Shenzhen Key Laboratory of Ultrafast Laser Micro/Nano Manufacturing, Key Laboratory of Optoelectronic Devices and Systems of Ministry of Education and Guangdong Province, College of Physics and Optoelectronic Engineering, Shenzhen University, Shenzhen 518060, China, and also with the Guangdong and Hong Kong Joint Research Centre for Optical Fiber Sensors, Shenzhen University, Shenzhen 518060, China (e-mail: 2210452029@email.szu.edu.cn; 874162079@qq.com; heyhhq2021@163.com; wjbao@szu.edu.cn; anmeliu@163.com; yingwang@szu.edu.cn; fucailing@szu.edu.cn; hejun07@szu.edu.cn; cliao@szu.edu.cn).

Yiping Wang is with the Guangdong Laboratory of Artificial Intelligence and Digital Economy (SZ), Shenzhen 518107, China, and also with the Guangdong and Hong Kong Joint Research Centre for Optical Fiber Sensors, Shenzhen University, Shenzhen 518060, China (e-mail: ypwang@szu.edu.cn).

Color versions of one or more figures in this article are available at https://doi.org/10.1109/JLT.2024.3524416.

Digital Object Identifier 10.1109/JLT.2024.3524416

The femtosecond laser is widely employed in fabricating optical waveguides and related functional devices. Its notable characteristics include ultrashort pulse duration, ultrahigh peak intensity, and high flexibility when tuning its fabrication parameters [9], [10], [11]. By using a femtosecond laser, it is possible to induce permanent refractive index modulation within materials. Consequently, a femtosecond laser plays a crucial role in the fabrication of optical devices in materials such as glass [12], [13], single crystals [14], [15], and optical fibers [16], [17], [18]. In 2003, Mihailov et al. proposed the fabrication of Bragg gratings on non-photosensitive optical fibers using the femtosecond laser phase mask technique, demonstrating spectral characteristics similar to those achieved with ultraviolet phase masks [19]. During the inscription process, stress can be applied to the optical fiber to tune the Bragg wavelength, but the range is still limited. Additionally, the femtosecond laser Talbot interferometer methods for fabricating FBG exhibit excellent wavelength tunability [20]. FBGs with different periods are generated by altering the angle between two incident light beams. However, this method requires intricate adjustments to the spatial optical path, demanding high stability and precision.

The femtosecond laser direct writing technique, with its high flexibility in fabricating fiber Bragg gratings of various types and different wavelengths, has garnered significant attention. To date, four typical techniques utilizing a femtosecond laser for FBG fabrication have been proposed, including the point-by-point (PbP) method [21], the line-by-line method [22], the plane-by-plane method [23], and continuous core scanning technology [24]. Among these, the PbP inscription method is widely applied in FBG preparation due to its efficiency [25]. However, FBGs written through the PbP technique often exhibit significant insertion losses attributed to the highly localized refractive index modifications (RIMs) within the fiber core [26], [27]. According to reports, the use of the slit beam shaping method has been effective in extending the width of the RIM region, thereby enabling the fabrication of high-quality FBGs [28]. However, there is a significant loss of laser energy after passing through the narrow slit. Moreover, adaptive slit based on Spatial Light Modulators (SLM) demonstrate greater flexibility in controlling laser energy and slit orientation. However, the experimental setup consisting of a 4f system is more complicated [29]. To address this issue, Li et al. proposed the utilization of a high-refractive-index-matching oil with the optical fiber to form a planoconcave cylindrical lens, effectively extending the width of the RIM region without the need for additional beam shaping devices [30]. Nevertheless, this method cannot be applied to strip waveguides.

In this study, we employed, for the first time, the femtosecond laser Burst-Mode method to fabricate high-quality WBGs in a PLC. This approach significantly reduces the number of reflection subpeaks, and the intensity of reflection subpeaks is also effectively suppressed, achieving a return loss as high as 32.74 dB. We also investigated the application of the Burst-Mode method in conjunction with a geometric apodization technique to fabricate double-apodized WBGs. This method effectively suppresses the sidelobes, achieving a maximum side-mode suppression ratio (SMSR) of 18.24 dB. Additionally, we investigated the fabrication of a pair of stress waveguides on both sides of the core in the PLC using a femtosecond laser, resulting in the WBG exhibiting low birefringence of $5.66 \times 10^{-6}$ and a low polarization-dependent loss (PDL) of 0.8 dB. Therefore, the proposed fabrication method can be used to inscribe high-quality WBGs in a PLC with potential applications in diverse fields, including optical communication systems, multi-parameter sensing, and fiber lasers.

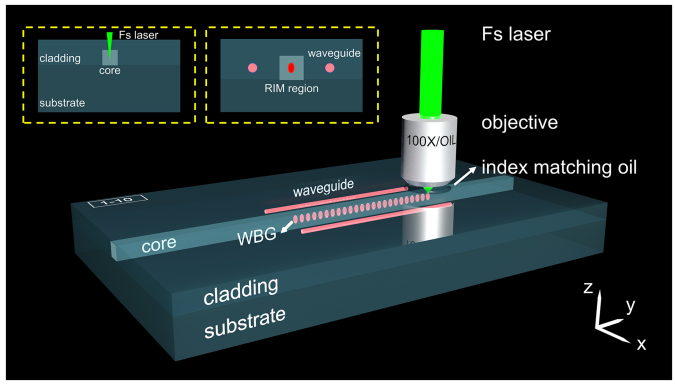


Fig. 1. Schematic of a WBG created in the PLC by femtosecond laser direct writing.

## II. Results and Discussion

### A. Setup of Fabrication PLC-WBG

The apparatus for inscribing WBGs into PLCs through femtosecond laser direct writing is depicted in Fig. 1. The system utilizes a frequency-doubled, regenerative amplified Yb: KGW femtosecond laser (Pharos, Light-conversion), which emits at a wavelength of 513 nm. The laser features a pulse width of 290 fs and operates at a repetition rate of 200 kHz. Focusing is achieved using a 100× oil-immersion objective lens, with refractive index matching oil applied to mitigate aberrations. To guarantee precision in the fabrication process, the PLC is securely positioned within a specialized holder affixed to an air-bearing stage, ensuring stability and accuracy. The fabrication of the WBG commences with the PLC undergoing a consistent translational motion following a meticulously defined trajectory. This movement aligns the PLC in such a way that the focused laser pulses systematically induce periodic RIM within the core material, leading to the formation of the WBG. Following the creation of the WBG, the PLC continues its translational motion along the same trajectory, with the focused laser now targeting the cladding region to establish stress waveguides. This comprehensive approach ensures the high-precision inscription of functional and structurally sound WBGs within the PLC framework.

### B. Minimizing the Insertion Loss and Reflection Subpeaks of PLC-WBG

Our study focused on understanding how the order of gratings influences the spectral response of WBGs within PLCs, a factor critical to the quality of the reflected spectrum. We fabricated a

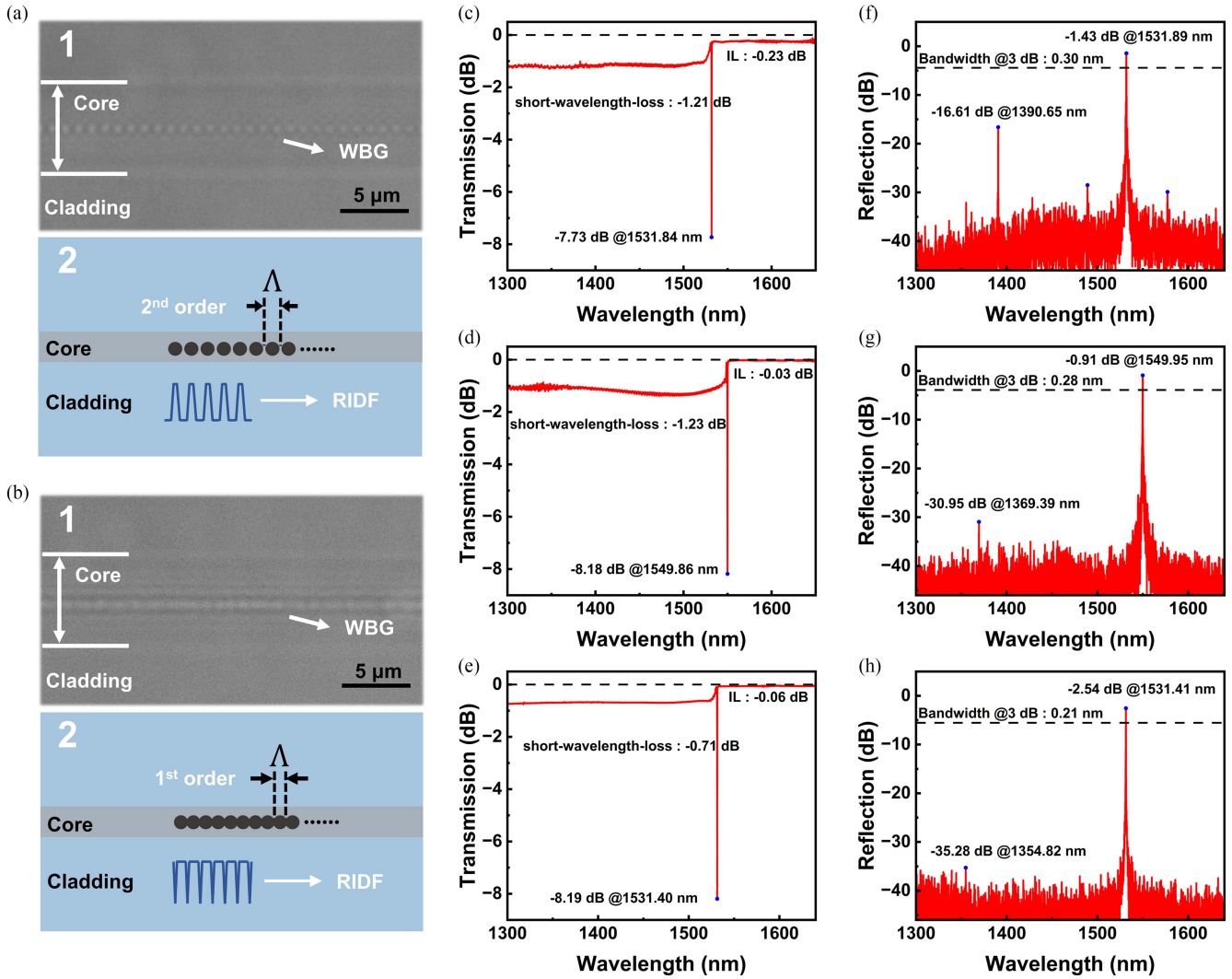


Fig. 2. Femtosecond laser PbP method for fabricating PLC-WBGs. (a) Panels 1 and 2 show the Top-view microscopic image and the refractive index distribution function (RIDF) schematic of the second-order WBG fabricated using the PbP method, corresponding to (c) transmission spectrum and (f) reflection spectrum. (b) Panels 1 and 2 show the Top-view microscopic image and the RIDF schematic of the first-order WBG fabricated using the PbP method, corresponding to (d) transmission spectrum and (g) reflection spectrum. (e), (h) transmission and reflection spectra of the first-order WBG fabricated using the Burst-Mode method, respectively.

second-order WBG utilizing the femtosecond laser PbP technique, characterized by a grating period of 1.058 $\mu$m and a total length of 5.5 mm. The fabrication parameters included a pulse energy setting of 16.9 nJ, yielding a Bragg resonance attenuation of 7.73 dB. The top-view microscope imagery and the transmission spectrum of this specimen are presented in Fig. 2(a1) and (c), respectively.

The WBG exhibited an insertion loss of 0.23 dB, with a short-wavelength loss of 1.21 dB. This phenomenon is primarily attributed to the relatively limited RIM area produced by the PbP method. Achieving high reflectivity in WBGs might necessitate elevated pulse energy or extended grating lengths, which could inflict considerable damage to the core, thereby escalating the insertion losses. Moreover, the use of a high numerical aperture (NA) oil-immersion microscope objective during fabrication concentrated the modifications highly localized within the PLC core. This localization heightens the propensity for coupling with cladding modes, further increasing additional insertion losses in short-wavelength.

The sample exhibited multiple reflection subpeaks throughout the spectrum, considerably diminishing the return loss, as illustrated in Fig. 2(f). Our analysis revealed that the low return loss associated with the second-order WBGs inscribed via the PbP method stems from the confined modulation region within the PLC core, where portions of the waveguide remain unmodulated. Consequently, the axial refractive index distribution function (RIDF) appears as a square wave-like modulation (Fig. 2(a2)). Such a refractive index modulation profile leads to the creation of multiple reflective interfaces within the core, manifesting as numerous reflection peaks across the spectrum. This effect directly impacts the grating's overall return loss, underscoring the critical role of grating order and fabrication parameters in defining the performance characteristics of PLC-WBGs.

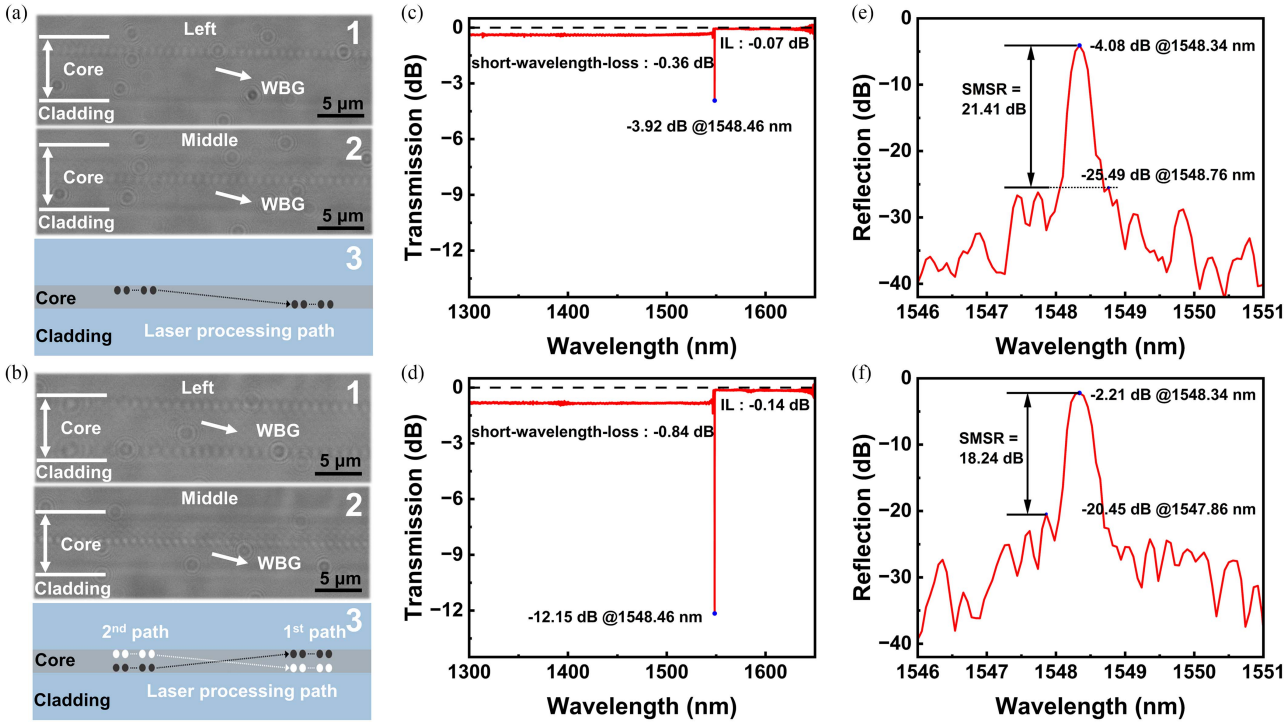


Fig. 3. Femtosecond laser Burst-Mode method for fabricating apodized WBGs. (a) Panels 1 and 2 show the Top-view microscopic images of the left and middle positions of the single-apodized WBG fabricated using the Burst-Mode method, along with (3) a schematic of the grating fabrication, corresponding to (c) transmission spectrum and (e) reflection spectrum. (b) Panels 1 and 2 show the Top-view microscopic images of the left and middle positions of the double-apodized WBG fabricated using the Burst-Mode method, along with (3) a schematic of the grating fabrication, corresponding to (d) transmission spectrum and (f) reflection spectrum.

In our endeavor to reduce the RIM gap and improve the spectral response of WBGs in PLCs, we opted for a first-order grating characterized by a smaller grating period. A femtosecond laser, set to a pulse energy of 13.16 nJ, inscribed a WBG with a grating period of 0.536 $\mu$m and a total length of 5.5 mm into the PLC. Fig. 2(b1) and (d) present the top-view microscopic image and transmission spectrum of the fabricated grating, respectively. The WBG exhibited a short-wavelength loss of 1.23 dB, with an insertion loss of merely 0.03 dB. This represents a substantial improvement over the second-order WBG, attributed to the first-order grating's enhanced coupling efficiency. As displayed in Fig. 2(g), although the PbP method for fabricating a first-order WBG demonstrated an ability to reduce the occurrence of multiple reflective subpeaks, it did not entirely eliminate reflection subpeaks throughout the entire spectrum. Specifically, a persistent reflection subpeak exceeding $-32$ dB intensity was observed near 1370 nm.

The challenge in completely eliminating reflection subpeaks across the spectrum stems from the inherent characteristics of the first-order grating. Its period, aiming for the same reflective wavelength, is half that of the second-order grating. Given the femtosecond laser direct writing's single-point diameter of approximately 900 nm, the RIM regions induced by the laser overlap. This overlap results in unequal modulation quantities within the overlapping areas, leading to an axial RIDF resembling a square wave-like modulation with an expanded duty cycle, as illustrated in Fig. 2(b2). While this approach successfully reduces the number of reflective subpeaks, the presence of unequal modulation in the overlap regions poses a challenge in fully suppressing these subpeaks across the spectrum.

In the quest to mitigate core damage and its consequential impact on device performance, our research introduces an innovative approach: the utilization of lower pulse energy with repeated exposures at the same location. This strategy minimizes the permanent damage inflicted by laser pulses on the core, while simultaneously accumulating sufficient single-point modulation to achieve the desired reflectivity. Herein, we advocate for the femtosecond laser Burst-Mode method as an optimal technique for fabricating PLC-WBGs.

In this novel approach, each period of the WBG is subjected to multiple exposures, allowing for a meticulous and controlled modulation of the refractive index without exacerbating core damage. We successfully inscribed a first-order WBG with a grating period of 0.529 $\mu$m and a total length of 6 mm into the PLC core. The transmission and reflection spectra of this sample are depicted in Fig. 2(e) and (h), respectively. The fabricated grating exhibited a Bragg resonance attenuation of 8.19 dB, demonstrating a remarkable control over additional insertion losses, the short-wavelength loss was 0.71 dB. Notably, the insertion loss was maintained below 0.1 dB, signifying a substantial improvement in minimizing core damage-related losses. A significant outcome of employing the Burst-Mode method is its effectiveness in diminishing the intensity of reflection subpeaks across the entire reflection spectrum. This is evidenced by the sample achieving a return loss of 32.74 dB, as showcased in Fig. 2(h).

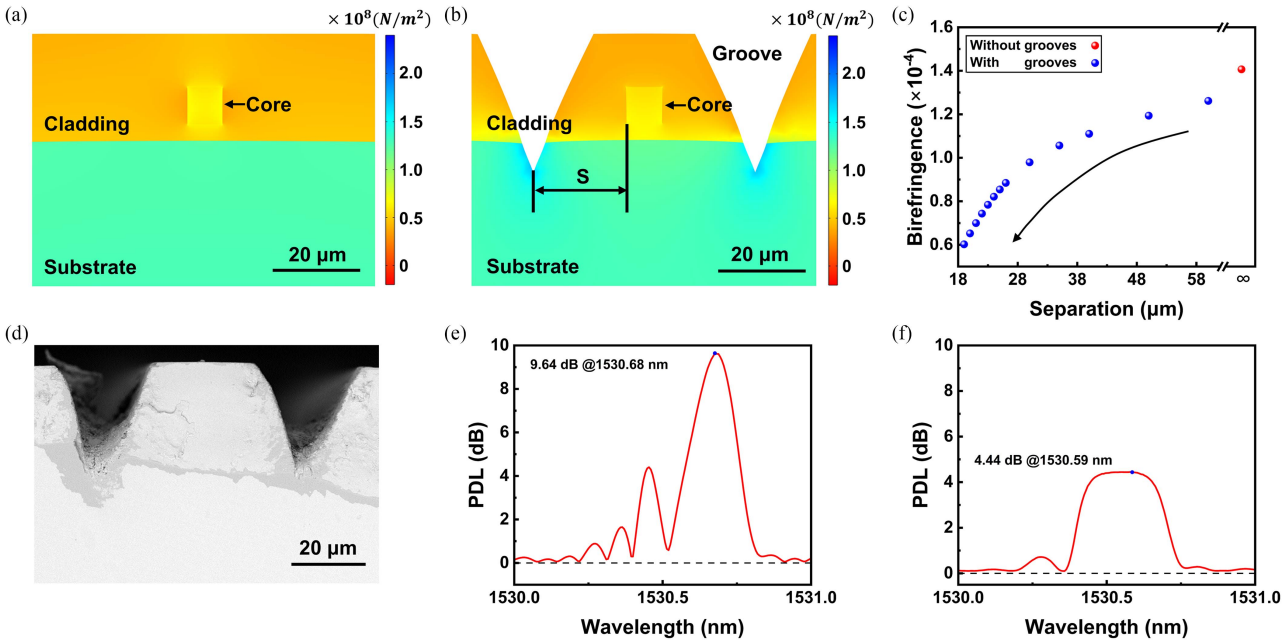


Fig. 4. Introducing grooves on both sides of the core in the PLC. (a), (b) The simulated results of internal stress in the PLC without grooves and with grooves (groove to the core spacing of 19 $\mu$m). (c) The simulated birefringence as a function of groove separation. The Red dot at $\infty$ separation represents the reference birefringence measured for a single WBG without grooves. (d) The cross-sectional SEM image of the grooves created in the PLC using a femtosecond laser. The PDL spectra for WBGs (e) without grooves and (f) with grooves.

### C. Optimizing the SMSR of PLC-WBG

In optimizing the SMSR for WBGs within PLCs, we embraced a novel strategy by combining the femtosecond laser Burst-Mode technique with a geometric apodization method to construct apodized Bragg gratings. This section details our methodological approach and outcomes, highlighting the enhanced performance achieved through these innovations.

Our initial endeavor involved fabricating a single-apodized Bragg grating. By precisely adjusting the femtosecond laser's scanning path, we introduced a unique apodization function, as illustrated in Fig. 3(a3). The fabricated grating, characterized by a 1.070 $\mu$m period and a 6 mm length, was strategically offset by 6 $\mu$m in the radial direction at both the front and end within the core. Setting the pulse energy at 16.25 nJ, we observed the grating's transmission and reflection spectra (Fig. 3(c) and (e), respectively), where the Bragg resonance attenuation reached 3.92 dB and a high SMSR of 21.41 dB was achieved due to the grating's lower reflectivity. The geometric apodization's practical implementation is visually demonstrated through the top-view microscopic images at the left and middle positions of the PLC-WBG (Fig. 3(a1) and (a2)). This technique modulates the grating's central portion directly onto the core's center, optimizing the overlap integral in the axial direction for maximum reflectance. Consequently, both ends of the grating experience a reduced equivalent modulation amount compared to its central part, creating a quasi-Gaussian apodization function. However, attaining high grating reflectance while maintaining an elevated SMSR proved challenging due to the intricacies of applying the femtosecond laser Burst-Mode method with geometric apodization.

To surmount this challenge, we innovated a dual-apodization approach by fabricating two Bragg gratings within the core, both featuring identical apodization amplitudes and periods, as depicted in Fig. 3(b3). This dual grating structure, designed with symmetric femtosecond laser scanning paths around the core's center axis, facilitated an overlap in the grating's central region, enabling the creation of a double-apodized grating with enhanced reflectance. The transmission and reflection spectra of this advanced double-apodized Bragg grating are showcased in Fig. 3(d) and (f), respectively. By maintaining consistent fabrication parameters, this grating exhibited an improved reflectance, evidenced by a Bragg resonance attenuation of 12.15 dB and an SMSR of 18.24 dB. Fig. 3(b1) and (b2) elucidate the dual femtosecond laser modulation paths symmetrically aligned with the core's central axis, with a significant overlap in the central grating region.

The employment of the femtosecond laser Burst-Mode method in tandem with geometric apodization for the creation of single and double-apodized Bragg gratings marks a significant advancement in PLC-WBG fabrication. This approach not only enhances the grating's reflectance but also effectively optimizes its SMSR, illustrating the potential for high-performance PLC-WBGs in various applications.

### D. Minimizing the PDL of PLC-WBG

Addressing the PDL in WBGs is crucial for their application in optical fiber communication. The inherent internal stress and core asymmetry in PLCs introduce significant birefringence effects, leading to undesirable drifts in the WBG's central wavelength with changes in the input optical polarization state.

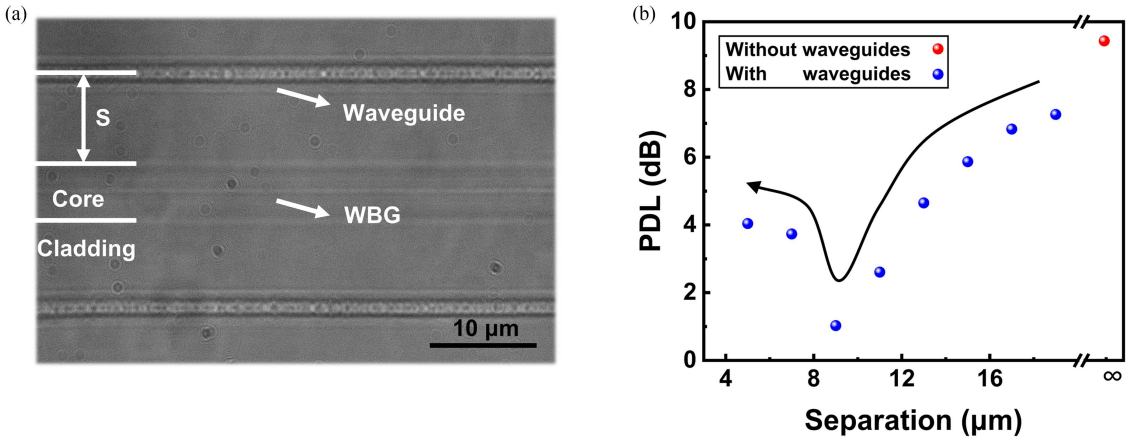


Fig. 5. Femtosecond laser fabrication of stress waveguides in the PLC. (a) Top-view microscopic image. (b) Birefringence as a function of the stress waveguide separation.

Consequently, enhancing the stability of the WBG and achieving low PDL are essential objectives for optimizing the performance of these optical components.

Our combined simulation and experimental studies indicate that the application of a femtosecond laser to etch grooves on both sides of the PLC core effectively reduces core birefringence and, by extension, the PDL of the WBG. The necessity for high-temperature annealing during PLC fabrication, due to the mismatch in thermal expansion coefficients (TEC) between the substrate and the cladding, exacerbates internal stress at operational temperatures. This stress leads to an anisotropic and inhomogeneous refractive index distribution within the core, primarily through the photoelastic effect. To quantify the impact of groove-induced stress relief in PLCs, we utilized COMSOL Multiphysics to simulate models with varying groove-to-core separation distances (19-60 $\mu$m). The simulation parameters were aligned with those employed in actual PLC fabrication processes, including a PLC material density of 2203 kg/m$^3$, a Young's modulus of 78 GPa, a Poisson ratio of 0.17, and a substrate TEC higher than that of the cladding.

The introduction of grooves led to a reduction in internal stress within the core from $7.39 \times 10^7$ N/m$^2$ to $5.92 \times 10^7$ N/m$^2$, as evidenced by the data in Fig. 4(a) and (b). A notable correlation between the groove separation distance and the core's birefringence was observed (Fig. 4(c)). Specifically, decreasing the separation distance to 19 $\mu$m resulted in the birefringence dropping from $1.41 \times 10^{-4}$ to $6.02 \times 10^{-5}$, effectively halving the birefringence induced by internal stress. An SEM image showcasing the femtosecond laser-etched grooves (Fig. 4(d)) reveals a groove width of approximately 26.5 $\mu$m and a depth of about 25 $\mu$m. Crucially, the application of these grooves led to a significant decrease in WBG-PDL from 9.64 dB to 4.44 dB, as shown in Fig. 4(e) and (f).

Utilizing the precision of femtosecond laser direct writing, we fabricated a pair of stress waveguides, each extending 6 mm in length, positioned symmetrically on either side of the PLC core. These waveguides are specifically engineered to induce controlled stress within the core, aiming to counteract the birefringence effects detrimental to the WBG's performance.

The top-view microscopic image, depicted in Fig. 5(a), illustrates the spatial configuration of the stress waveguides relative to the core, with the separation marked as S. Fig. 5(b) provides a comprehensive analysis of the PDL variation as a function of the stress waveguide separation (S) from the core. Additionally, it includes a comparison with the reference WBG-PDL at infinite separation (absence of stress waveguides), serving as a baseline for each fabrication condition. Our findings reveal a pivotal trend: for separation spacings greater than 9 $\mu$m, a reduction in the distance between the stress waveguide and the core correlates with a decrease in the WBG's PDL. However, spacings of less than 9 $\mu$m lead to an increase in PDL, attributable to the stress from the waveguides exceeding an optimal threshold, thus causing "overcompensation" in the stress dynamics within the core.

The strategic application of femtosecond laser-fabricated stress waveguides effectively minimized the WBG's PDL from 9.43 dB to an impressively low value of 1.03 dB. This significant improvement underscores the potential of precise stress modulation techniques in overcoming the inherent challenges posed by birefringence in PLC-based optical components.

Next, we analyze the reduction of WBG-PDL in a PLC caused by stress waveguides from the perspective of waveguide birefringence. The waveguide birefringence, $\Delta n_B = n_V - n_H$ [31], was calculated from the Bragg wavelength splitting between two orthogonal linear polarization modes as described in [32], using (1), where $\Delta\lambda_B$ is the separation between the Bragg resonances of the two orthogonal linear polarization and $\Lambda$ is the periodicity of the Bragg grating.

$$\Delta n_B = \Delta\lambda_B / \Lambda \tag{1}$$

The simulation results of internal stress in the PLC, shown in Fig. 4(a), and the schematic cross-sectional diagram of the PLC in Fig. 6(a) reveal that the presence of internal stress and structural asymmetry in the PLC (such as the asymmetry in the rectangular core and cladding width) introduces high birefringence. The cross-sectional schematic diagram of the RIM region of the WBG prepared by the femtosecond laser Burst-Mode method is shown in Fig. 6(b). Due to the femtosecond laser acting on the core, there is positive and negative

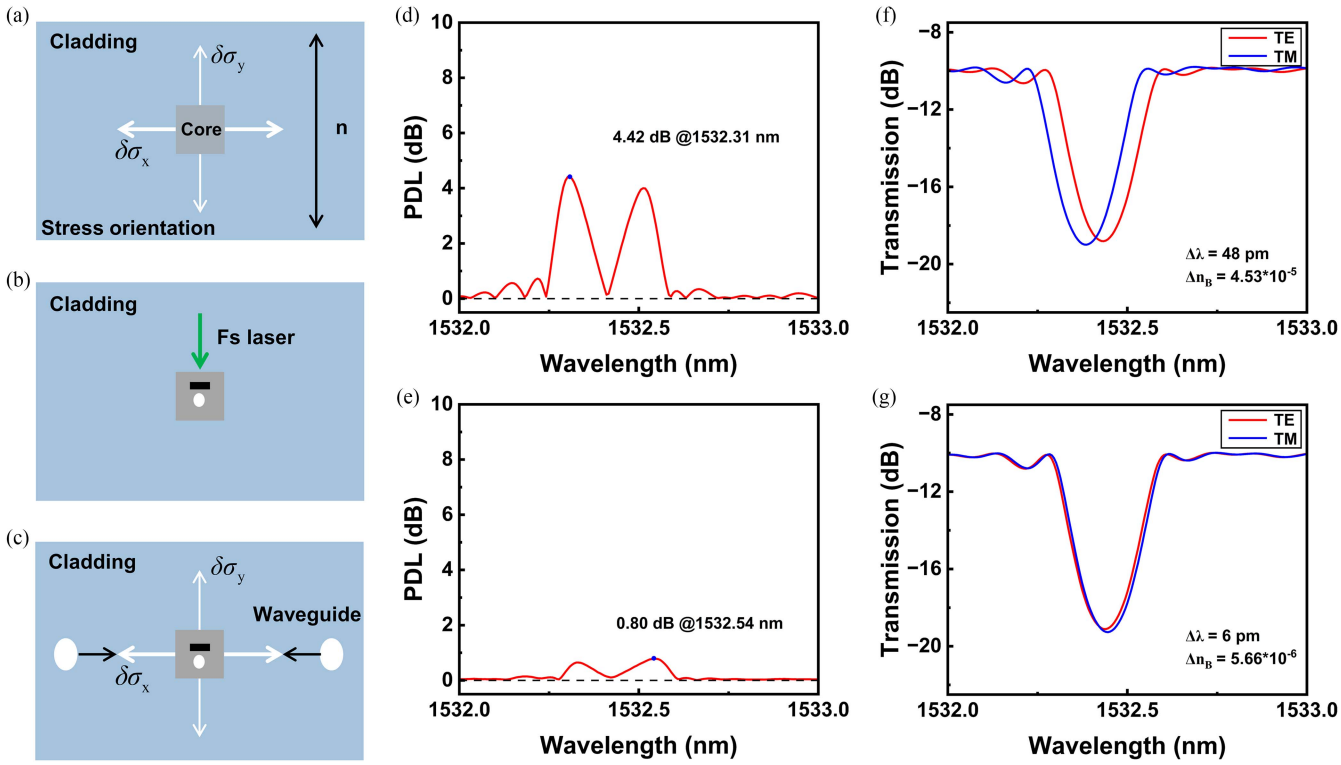


Fig. 6. Analysis of femtosecond laser-induced stress waveguide fabrication for effectively reducing the PDL of WBG. (a)–(c) Cross-sectional diagram of the internal stress of the core, WBG inscribed on the core, and stress waveguides inscribed on both sides of the core. (d), (f) PDL spectra and transmission spectra of two orthogonal linear polarization modes (i.e., TE and TM) for PLC-WBG (without stress waveguides). (e), (g) PDL spectra and transmission spectra of two orthogonal linear polarization modes (i.e., TE and TM) for PLC-WBG (with stress waveguides).

RIM as well as asymmetry in the modulation region [33], [34]. This introduces birefringence, thereby compensating for the PDL of the PLC-WBG. We employed a Mueller-matrix-based commercial polarization analysis system to measure the polarization-resolved transmission spectra and PDL spectra of the WBG, which consists of a tunable laser (Agilent, 81940A), a polarization synthesizer (Agilent, N7786B), and an optical power meter (Agilent, N7744A). As shown in Fig. 6(d) and (f), the Burst-Mode WBG exhibits a PDL of 4.42 dB, with a Bragg wavelength difference (i.e., $\Delta\lambda_B$) is 0.048 nm between two orthogonal linear polarization modes (i.e., TE and TM). Using the Formula (1), the birefringence was calculated to be $4.53 \times 10^{-5}$. Finally, stress waveguides were inscribed on both sides of the core in the PLC using a femtosecond laser, as shown in Fig. 6(c). By applying stress to the core through the stress waveguides, the birefringence of the PLC-WBG was measured to be $5.66 \times 10^{-6}$, with a PDL of 0.8 dB, as displayed in Fig. 6(e) and (g). Thus, significant optimization in the PDL of the WBG inscribed in the PLC was achieved.

## III. Conclusion

We demonstrated the fabrication of high-quality WBGs in a PLC using femtosecond laser technology. We investigated the Burst-Mode method for fabricating first-order WBGs, which significantly reduces the number of reflection subpeaks and suppresses reflection subpeak intensity to as low as 35.28 dB, achieving a return loss of 32.74 dB. We also investigated the application of the Burst-Mode method in conjunction with a geometric apodization technique to fabricate double-apodized WBGs. This approach ensures a Bragg resonance attenuation of 12.15 dB while achieving a maximum SMSR of 18.24 dB. Additionally, we investigated the fabrication of stress waveguides on both sides of the core engraved with WBGs in the PLC using a femtosecond laser, serving as stressors. The resulting WBG exhibits a low birefringence of $5.66 \times 10^{-6}$ and a low PDL of 0.8 dB. These improvements in WBG performance and reliability are pivotal for the ongoing development of sophisticated optical devices, setting a new benchmark for PLC technology in various scientific and industrial applications.

## References

[1] R. Guo et al., "High–bit rate ultra-compact light routing with mode-selective on-chip nanoantennas," *Sci. Adv.*, vol. 3, no. 7, Jul. 2017, Art. no. e1700007, doi: 10.1126/sciadv.1700007.

[2] G. Calafiore et al., "Holographic planar lightwave circuit for on-chip spectroscopy," *Light-Sci. Appl.*, vol. 3, no. 9, Sep. 2014, Art. no. e203, doi: 10.1038/lsa.2014.84.

[3] J. You, Y. Wang, Q. Han, and J. An, "Silica-silicon based planar lightwave circuit quantum key distribution decoding chip for multi-protocol," *Opt. Laser Technol.*, vol. 145, Jan. 2022, Art. no. 107505, doi: 10.1016/j.optlastec.2021.107505.

[4] R. K. Kim, J. H. Lim, J. H. Song, and K. S. Lee, "Highly linear-polarized external cavity lasers hybrid integrated on planar lightwave circuit platform," *IEEE Photon. Technol. Lett.*, vol. 18, no. 4, pp. 580–582, Feb. 2006, doi: 10.1109/LPT.2006.870141.

[5] K. S. Lee et al., "Dual-wavelength external cavity laser with a sampled grating formed in a silica PLC waveguide for terahertz beat signal generation," *Appl. Phys. B-Laser Opt.*, vol. 87, no. 2, pp. 293–296, Apr. 2007, doi: 10.1007/s00340-007-2600-3.
[6] J. H. Song, K. S. Lee, and Y. Oh, "Triple wavelength demultiplexers for low-cost optical triplexer transceivers," *J. Lightw. Technol.*, vol. 25, no. 1, pp. 350–358, Jan. 2007, doi: 10.1109/JLT.2006.886714.
[7] X. Zhang, F. Lu, S. Chen, X. Zhao, M. Zhu, and X. Sun, "Remote coding scheme based on waveguide Bragg grating in PLC splitter chip for PON monitoring," *Opt. Exp.*, vol. 24, no. 5, pp. 4351–4364, Mar. 2016, doi: 10.1364/OE.24.004351.
[8] J. Rathje, M. Kristensen, and J. E. Pedersen, "Continuous anneal method for characterizing the thermal stability of ultraviolet Bragg gratings," *J. Appl. Phys.*, vol. 88, no. 2, pp. 1050–1055, Jul. 2000, doi: 10.1063/1.373775.
[9] L. Li, W. Kong, and F. Chen, "Femtosecond laser-inscribed optical waveguides in dielectric crystals: A concise review and recent advances," *Proc SPIE*, vol. 4, no. 2, Mar. 2022, Art. no. 024002, doi: 10.1117/1.AP.4.2.024002.
[10] J. Shi, R. Chen, and X. Feng, "Short-length nanosecond pulsed 1.653-$\mu$m DBR fiber Raman laser oscillator fabricated by femtosecond laser direct-writing," *Opt. Laser Technol.*, vol. 180, Jan. 2025, Art. no. 111433, doi: 10.1016/j.optlastec.2024.111433.
[11] A.-L. Viotti et al., "Multi-pass cells for post-compression of ultrashort laser pulses," *Optica*, vol. 9, no. 2, pp. 197–216, Feb. 2022, doi: 10.1364/OPTICA.449225.
[12] J. Lu et al., "Tailoring chiral optical properties by femtosecond laser direct writing in silica," *Light-Sci. Appl.*, vol. 12, no. 1, p. 46, Feb. 2023, doi: 10.1038/s41377-023-01080-y.
[13] M. Sakakura, Y. Lei, L. Wang, Y.-H. Yu, and P. G. Kazansky, "Ultralow-loss geometric phase and polarization shaping by ultrafast laser writing in silica glass," *Light-Sci. Appl.*, vol. 9, no. 1, p. 15, Feb. 2020, doi: 10.1038/s41377-020-0250-y.
[14] F. Chen and J. R. V. De Aldana, "Optical waveguides in crystalline dielectric materials produced by femtosecond-laser micromachining," *Laser Photon. Rev.*, vol. 8, no. 2, pp. 251–275, Mar. 2014, doi: 10.1002/lpor.201300025.
[15] J. He et al., "Femtosecond laser plane-by-plane inscription of Bragg gratings in sapphire fiber," *J. Lightw. Technol.*, vol. 41, no. 22, pp. 7014–7020, Nov. 2023, doi: 10.1109/JLT.2023.3294794.
[16] H. Li et al., "Femtosecond laser fabrication of large-core fiber Bragg gratings for high-power fiber oscillators," *APL Photon.*, vol. 8, no. 4, Apr. 2023, Art. no. 046101, doi: 10.1063/5.0130238.
[17] A. Wolf et al., "Advances in femtosecond laser direct writing of fiber Bragg gratings in multicore fibers: Technology, sensor and laser applications," *Opto-Electron. Adv.*, vol. 5, no. 4, 2022, Art. no. 210055, doi: 10.29026/oea.2022.210055.
[18] Z. Cai et al., "Encrypted optical fiber tag based on encoded fiber Bragg grating array," *Int. J. Extreme Manuf.*, vol. 5, no. 3, Sep. 2023, Art. no. 035502, doi: 10.1088/2631-7990/acd825.
[19] S. J. Mihailov et al., "Fiber Bragg gratings made with a phase mask and 800-nm femtosecond radiation," *Opt. Lett.*, vol. 28, no. 12, pp. 995–997, Jun. 2003, doi: 10.1364/OL.28.000995.
[20] M. Becker et al., "Fiber Bragg grating inscription combining DUV subpicosecond laser pulses and two-beam interferometry," *Opt. Exp.*, vol. 16, no. 23, pp. 19169–19178, Nov. 2008, doi: 10.1364/OE.16.019169.
[21] G. D. Marshall, R. J. Williams, N. Jovanovic, M. J. Steel, and M. J. Withford, "Point-by-point written fiber-Bragg gratings and their application in complex grating designs," *Opt. Exp.*, vol. 18, no. 19, pp. 19844–19859, Sep. 2010, doi: 10.1364/OE.18.019844.
[22] K. Zhou, M. Dubov, C. Mou, L. Zhang, V. K. Mezentsev, and I. Bennion, "Line-by-line fiber Bragg grating made by femtosecond laser," *IEEE Photon. Technol. Lett.*, vol. 22, no. 16, pp. 1190–1192, Aug. 2010, doi: 10.1109/LPT.2010.2050877.
[23] P. Lu et al., "Plane-by-plane inscription of grating structures in optical fibers," *J. Lightw. Technol.*, vol. 36, no. 4, pp. 926–931, Feb. 2018, doi: 10.1109/JLT.2017.2750490.
[24] R. J. Williams, R. G. Krämer, S. Nolte, and M. J. Withford, "Femtosecond direct-writing of low-loss fiber Bragg gratings using a continuous core-scanning technique," *Opt. Lett.*, vol. 38, no. 11, pp. 1918–1920, Jun. 2013, doi: 10.1364/OL.38.001918.
[25] B. Xu et al., "Femtosecond laser point-by-point inscription of an ultra-weak fiber Bragg grating array for distributed high-temperature sensing," *Opt. Exp.*, vol. 29, no. 20, pp. 32615–32626, Sep. 2021, doi: 10.1364/OE.437479.
[26] J. Thomas et al., "Cladding mode coupling in highly localized fiber Bragg gratings: Modal properties and transmission spectra," *Opt. Exp.*, vol. 19, no. 1, pp. 325–341, Jan. 2011, doi: 10.1364/OE.19.000325.
[27] J. U. Thomas et al., "Cladding mode coupling in highly localized fiber Bragg gratings II: Complete vectorial analysis," *Opt. Exp.*, vol. 20, no. 19, pp. 21434–21449, Sep. 2012, doi: 10.1364/OE.20.021434.
[28] X. Xu et al., "Slit beam shaping for femtosecond laser point-by- point inscription of high-quality fiber Bragg gratings," *J. Lightw. Technol.*, vol. 39, no. 15, pp. 5142–5148, Aug. 2021, doi: 10.1109/JLT.2021.3082566.
[29] P. S. Salter et al., "Adaptive slit beam shaping for direct laser written waveguides," *Opt. Lett.*, vol. 37, no. 4, pp. 470–472, Feb. 2012, doi: 10.1364/OL.37.000470.
[30] X. Li, F. Chen, W. Bao, R. Wang, and X. Qiao, "Beam-shaping device-free femtosecond laser plane-by-plane inscription of high-quality FBGs," *Opt. Laser Technol.*, vol. 161, Jun. 2023, Art. no. 109226, doi: 10.1016/j.optlastec.2023.109226.
[31] L. A. Fernandes, J. R. Grenier, P. R. Herman, J. S. Aitchison, and P. V. S. Marques, "Femtosecond laser writing of waveguide retarders in fused silica for polarization control in optical circuits," *Opt. Exp.*, vol. 19, no. 19, pp. 18294–18301, Sep. 2011, doi: 10.1364/OE.19.018294.
[32] L. A. Fernandes, J. R. Grenier, P. R. Herman, J. S. Aitchison, and P. V. S. Marques, "Femtosecond laser writing of polarization devices for optical circuits in glass," *Proc SPIE*, vol. 8247, Feb. 2012, Art. no. 82470M, doi: 10.1117/12.907517.
[33] J. Wu et al., "Optimized femtosecond laser direct-written fiber Bragg gratings with high reflectivity and low loss," *Opt. Exp.*, vol. 31, no. 3, pp. 3831–3838, Jan. 2023, doi: 10.1364/OE.482198.
[34] N. Jovanovic et al., "Polarization-dependent effects in point-by-point fiber Bragg gratings enable simple, linearly polarized fiber lasers," *Opt. Exp.*, vol. 17, no. 8, pp. 6082–6095, Apr. 2009, doi: 10.1364/OE.17.006082.

**Jiajun Guan** received the B.S. degree in optoelectronic information science and engineering from Foshan University, Foshan, China, in 2021. He is currently working toward the Postgraduation degree in optoelectronic information engineering with Shenzhen University, Shenzhen, China. His research interests include fiber gratings and femtosecond laser micromachining.

**Zhihao Cai** received the B.S. degree in measurement and control technology and instruments from Shenzhen University, Shenzhen, China, in 2020, and the master's degree in optical engineering from Shenzhen University.

**Haoqiang Huang** is currently working toward the Ph.D. degree with Shenzhen University under the supervision of Prof. Changrui Liao. His research focuses on the development of various advanced fiber-tip microstructure sensors with stimuli-responsive properties.

**Weijia Bao** received the B.S. degree in electronic information science and technology from Xidian University, Shaanxi, China, in 2013, and the Ph.D. degree in optics from Northwest University, Xi'an, China, in 2018. He is currently a Assistant Professor with the College of Physics and Optoelectronic Engineering, Shenzhen University, Shenzhen, China. His research interests include fiber grating inscription, micromaching, and fiber sensing technology.

**Dejun Liu** received the Ph.D. degree from Photonics Research Centre, Dublin Institute of Technology, Dublin, Ireland, in 2018. In 2018, he joined Shenzhen University, Shenzhen, China. He has authored or coauthored more than 50 papers in academic journals and international conferences so far. His research interests include fiber optic endoscopic imaging and fiber sensing technology.

**Ying Wang** received the B.Eng. degree in applied physics and the Ph.D. degree in physical electronics from the Huazhong University of Science and Technology, Wuhan, China, in 2004 and 2010. Since 2015, he has been with Shenzhen University as a Lecturer, Associate Professor and special Researcher.

**Cailing Fu** received the M.S. degree in optical engineering from the Wuhan Institute of Technology, Wuhan, China, in 2015, and the Ph.D. degree in optical engineering from Shenzhen University, Shenzhen, China, in 2018. From 2018 to 2020, she was with Information and Communication Engineering, Shenzhen University, as a Postdoc Research Fellow. In 2020, she joined Shenzhen University. Her research focuses on distributed optical fiber sensing technology.

**Jun He** (Member, IEEE) was born in Hubei, China, in 1985. He received the B.Eng. degree in electronic science and technology from Wuhan University, Wuhan, China, in 2006, and the Ph.D. degree in electrical engineering from the Institute of Semiconductors, Chinese Academy of Sciences, Beijing, China, in 2011. Since 2017, he has been with Shenzhen University, Shenzhen, China, as an Assistant Professor/Associate Professor/Professor. His research interests include optical fiber sensors, fiber Bragg gratings (FBGs), and fiber lasers.

**Yiping Wang** (Senior Member, IEEE) was born in Chongqing, China, in 1971. He received the B.Eng. degree in precision instrument engineering from the Xi'an Institute of Technology, Xi'an, China, in 1995, and the M.S. and Ph.D. degrees in optical engineering from Chongqing University, Chongqing, China, in 2000 and 2003, respectively. From 2003 to 2005, he was with Shanghai Jiao Tong University, Shanghai, China, as a Postdoctoral Fellow. From 2005 to 2007, he was with the Hong Kong Polytechnic University, Hong Kong, as a Postdoctoral Fellow. From 2007 to 2009, he was with the Institute of Photonic Technology, Jena, Germany, as a Humboldt Research Fellow. From 2009 to 2011, he was with the Optoelectronics Research Centre, University of Southampton, Southampton, U.K., as a Marie Curie Fellow. Since 2012, he has been with Shenzhen University, Shenzhen, China, as a Distinguished Professor. He has authored or coauthored one book, 21 patent applications, and more than 240 journal and conference papers. His research interests include optical fiber sensors, fiber gratings, and photonic crystal fibers. Prof. Wang is the Optical Society of America and the Chinese Optical Society.

**Changrui Liao** (Member, IEEE) received the B.Eng. degree in optical engineering and the M.S. degree in physical electronics from the Huazhong University of Science and Technology, Wuhan, China, in 2005 and 2007, respectively, and the Ph.D. degree in electrical engineering from Hong Kong Polytechnic University, Hong Kong, in 2012. Since 2013, he has been with Shenzhen University, Shenzhen, China, as an Assistant Professor/Associate/Professor. His research interests include Laser 3D nanolithography technology and its applications in smart healthcare, smart chips, and new energy.